Solvoselective effect of Cu-B_2O_3/porous boron nitride on catalytic conversion of arylboric acids to phenols and biphenyls

Yumei Zhang[a], Yue Wang[a], Dongle Wang[a], Yating Liu[a], Tong Gao[a], Qingqiang Zhou[a], Qingzhi Luo[a], Jing An[a], Xueyan Li[a], Yandong Duan[a,*], Desong Wang[a,b,*]

[a] *Hebei Key Laboratory of Photoelectric Control on Surface and Interface, School of Sciences, Hebei University of Science and Technology, Shijiazhuang 050018, People's Republic of China*

[*] *Corresponding authors. E-mail address: ydduan@iccas.ac.cn (Y. Duan)*

[b] *State Key Laboratory of Metastable Materials Science and Technology (MMST), Hebei Key Laboratory of Applied Chemistry, Yanshan University, Qinhuangdao 066004, People's Republic of China*

[*] *Corresponding authors. E-mail address: dswang06@126.com (D. Wang)*

Experimental Section

1. HPLC analysis method and yield calculation

The reaction progress was monitored, and the yields were quantified using high-performance liquid chromatography (HPLC) with an external standard method.

1.1 Phenol analysis:

Mobile phase: Methanol/Water = 7:3 (v/v)

Flow rate: 1.00 mL/min

Detection wavelength: 270 nm

Standard curve: A series of phenol solutions in water (1-5 g/L) were analyzed. The calibration curve was $y = 6.4805 \times 10^4 x$ (where y is the peak area and x is the concentration in g/L), with a correlation coefficient of $R^2 = 0.9944$ (Fig. S2).

1.2 Biphenyl analysis:

Mobile phase: Methanol/Water = 9:1 (v/v)

Flow rate: 1.00 mL/min

Detection wavelength: 254 nm

Standard curve: A series of biphenyl solutions in methanol (1-5 g/L) were analyzed. The calibration curve was $y = 2.33062 \times 10^5 x$, with a correlation coefficient of $R^2 = 0.9994$ (Fig. S3).

1.3 Yield calculation:

During the reaction, samples were periodically withdrawn, diluted, and analyzed by HPLC. The concentration of the product in the sample ($C_{calculated}$) was determined by substituting the measured peak area ($A_{unknown}$) into the corresponding standard curve equation ($C_{calculated} = A_{unknown} / k$, where k is the slope). The actual mass of the product (m_{actual}) was then calculated by considering the dilution factor (D). $m_{actual} = C_{calculated} \times V_{unknown} \times D_{unknown}$. The yield was finally calculated as: Yield (%) = ($m_{actual} / m_{theoretical}$) × 100%, where $m_{theoretical}$ is the theoretical mass of the product based on 100% conversion of the starting material.

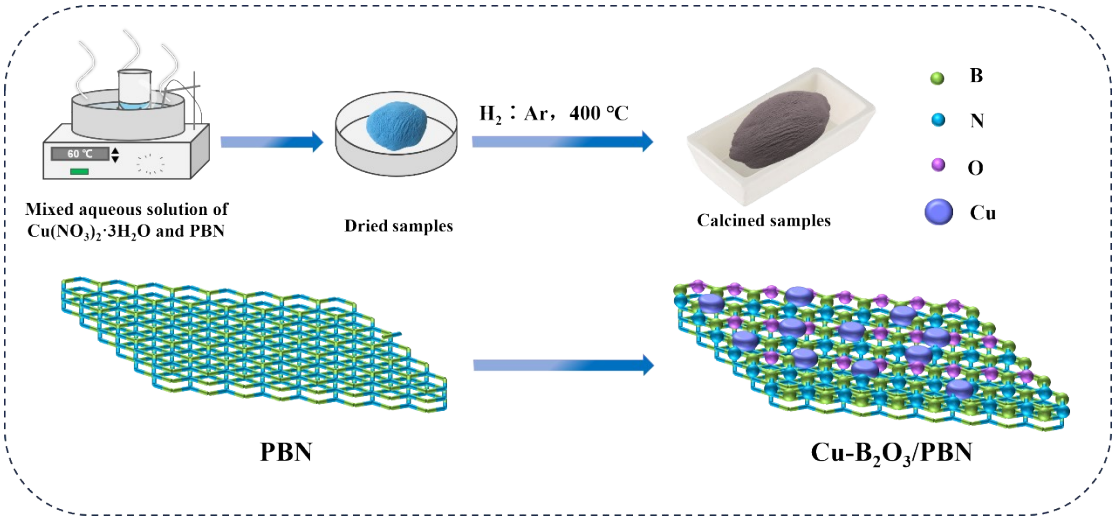

Fig. S1. Preparation process of Cu-B_2O_3/PBN nanocatalyst.

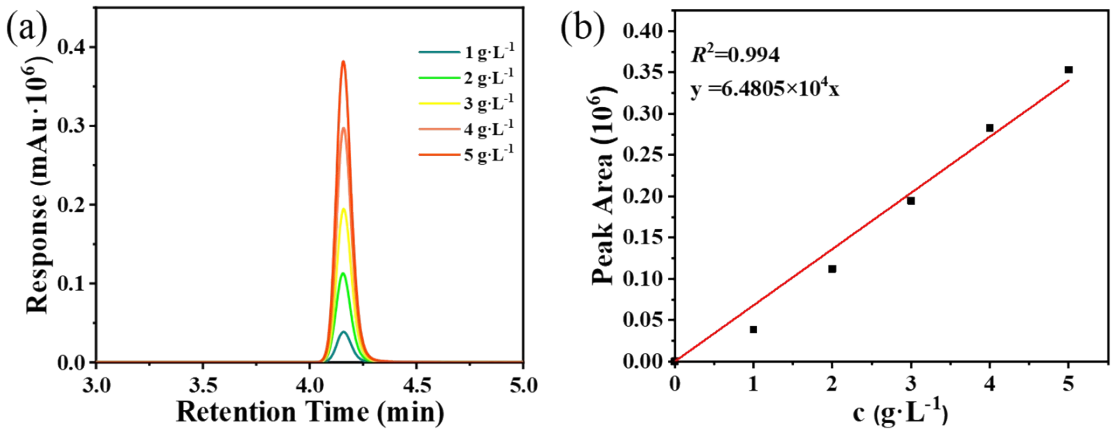

Fig. S2. (a) HPLC images of phenol solutions with different concentrations. (b) Standard curve of phenol solution obtained from (a) data.

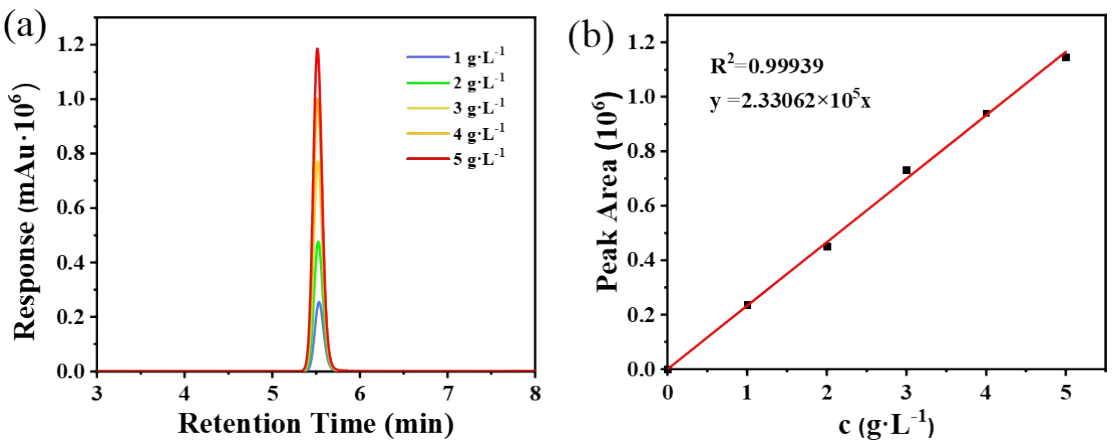

Fig. S3. (a) HPLC images of different concentrations of biphenyl in methanol solution. (b) Standard curve of biphenyl solution obtained from (a) data.

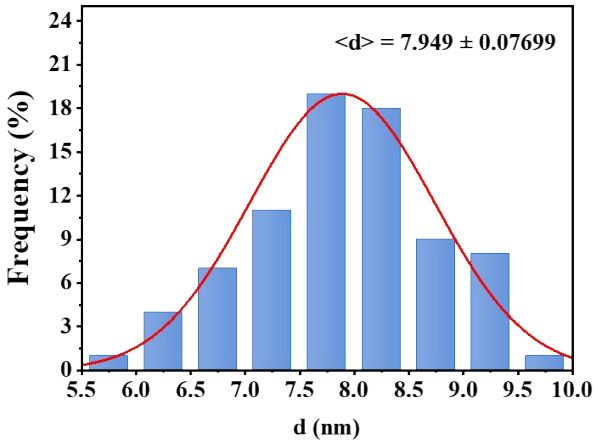

Fig. S4. Cu particle size distribution chart of Cu-B_2O_3/PBN.

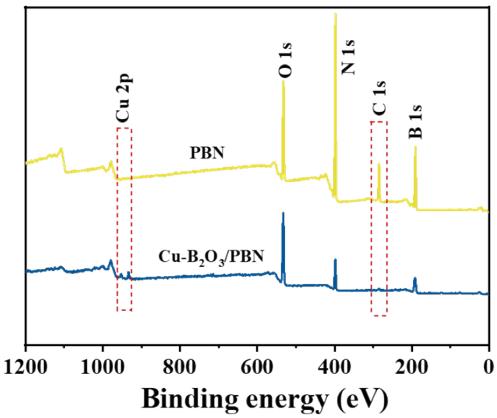

Fig. S5. Survey XPS spectra of PBN and the fresh Cu-B_2O_3/PBN.

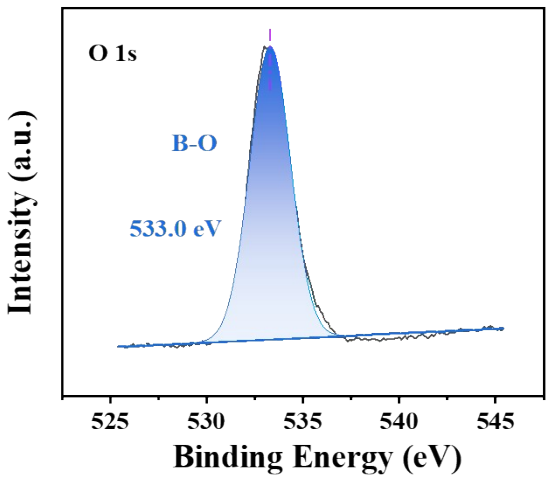

Fig. S6. O 1s XPS of PBN and Cu-B_2O_3/PBN.

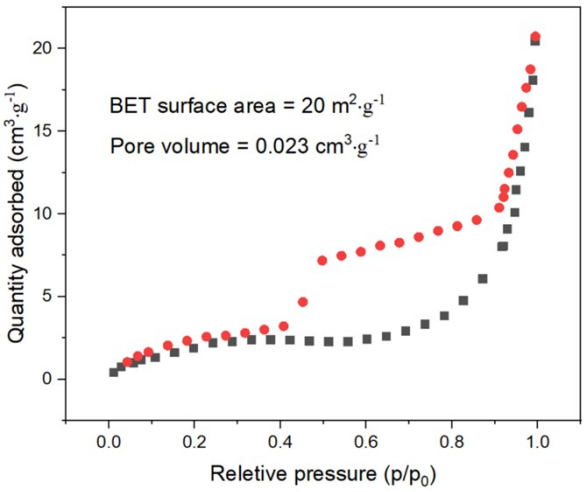

Fig S7. N_2 adsorption-desorption isotherm of Cu-B_2O_3/PBN.

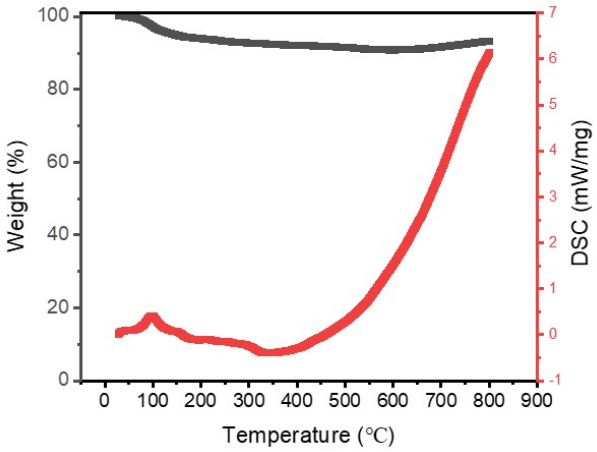

Fig. S8. TG and DSC curves of the Cu-B_2O_3/PBN.

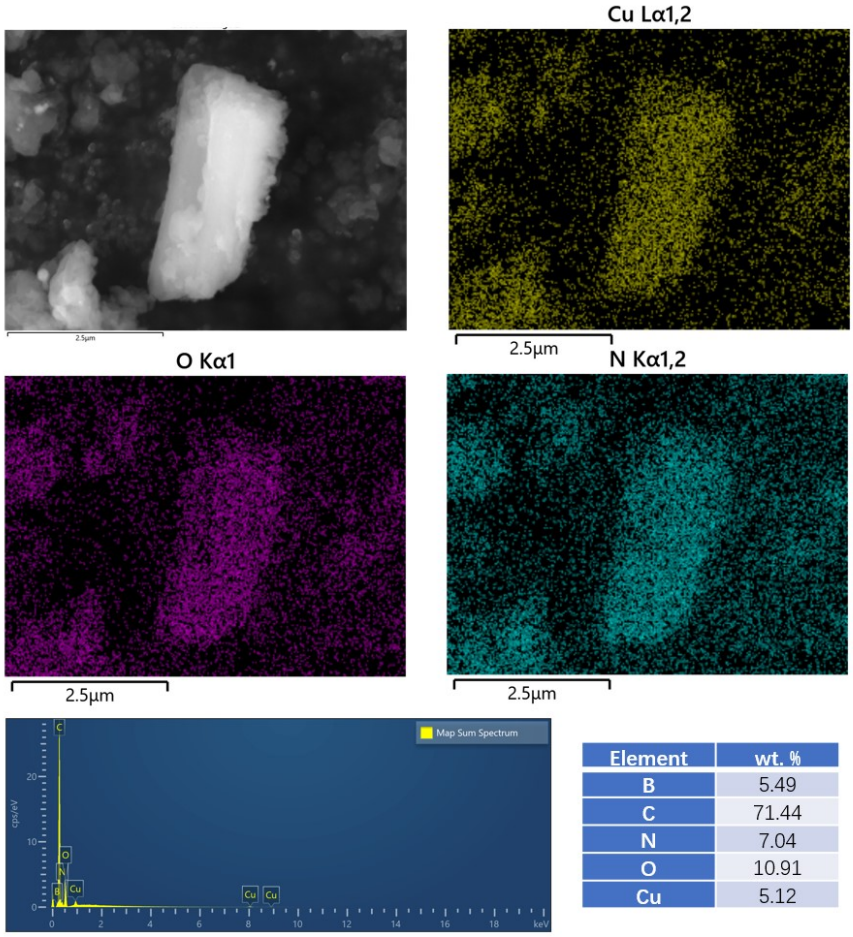

Element	wt. %
B	5.49
C	71.44
N	7.04
O	10.91
Cu	5.12

Fig. S9. FESEM image and EDAX analyses of the fresh Cu-B_2O_3/PBN.

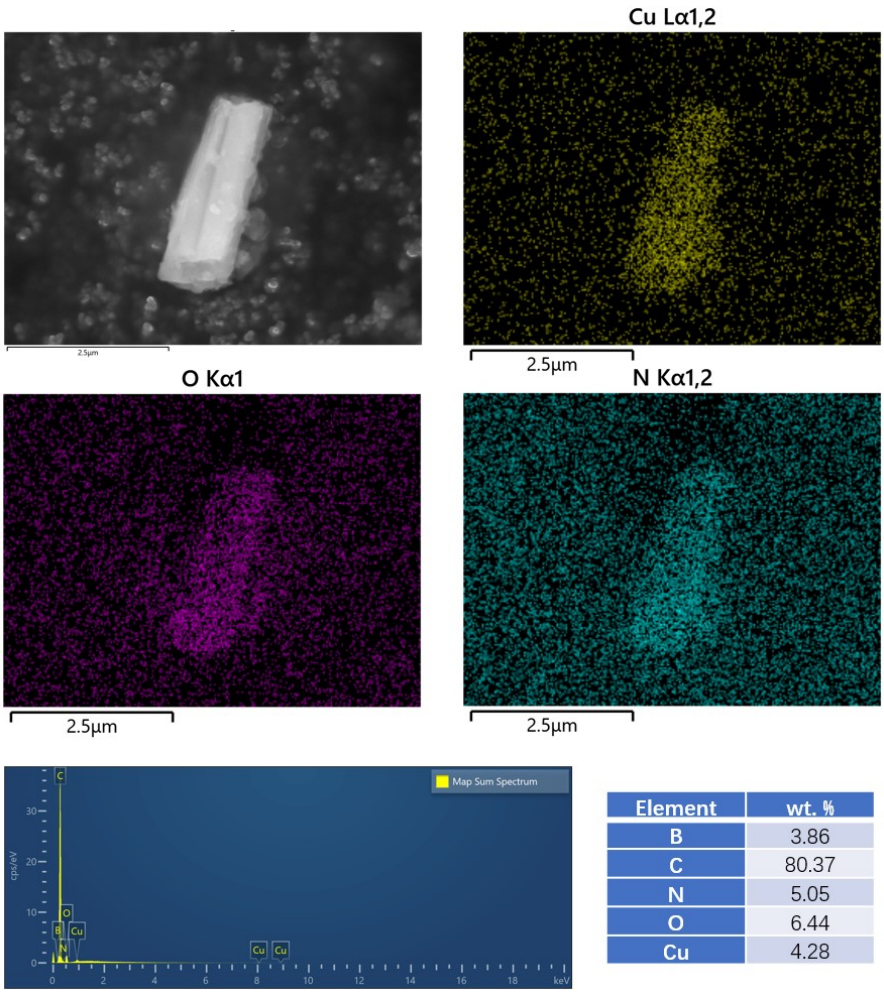

Element	wt. %
B	3.86
C	80.37
N	5.05
O	6.44
Cu	4.28

Fig. S10. FESEM image and EDAX analyses of the used Cu-B_2O_3/PBN (after six *ipso*-hydroxylation reaction cycles).

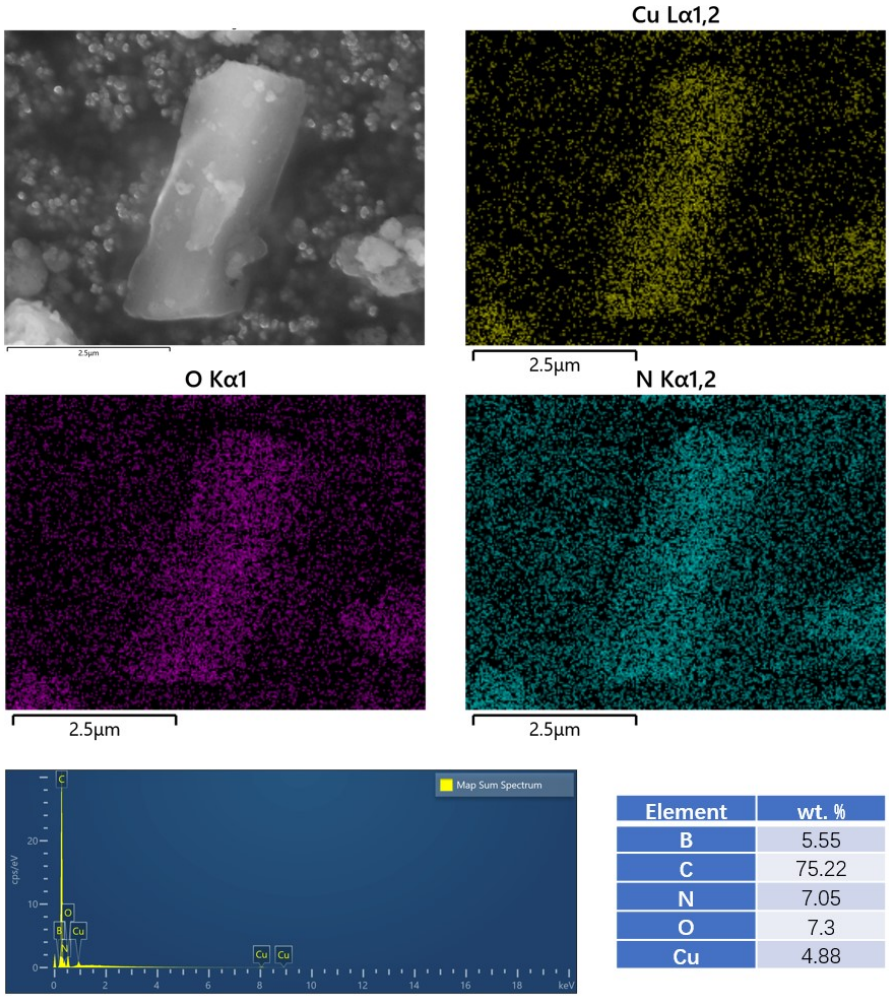

Element	wt. %
B	5.55
C	75.22
N	7.05
O	7.3
Cu	4.88

Fig. S11. FESEM image and EDAX analyses of the used Cu-B_2O_3/PBN (after six C-C homocoupling reaction cycles).

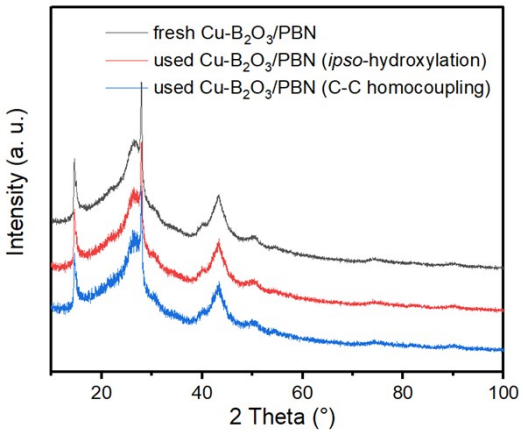

Fig. S12. XRD analyses of the fresh and used Cu-B_2O_3/PBN.

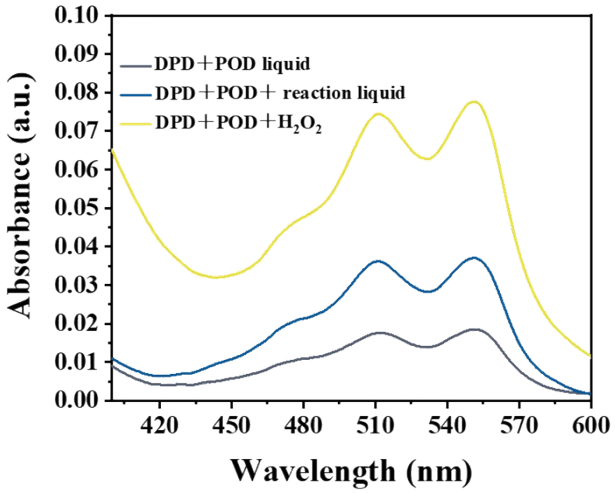

Fig. S13. The UV-Vis spectrum of detecting H_2O_2 in the reaction solution.

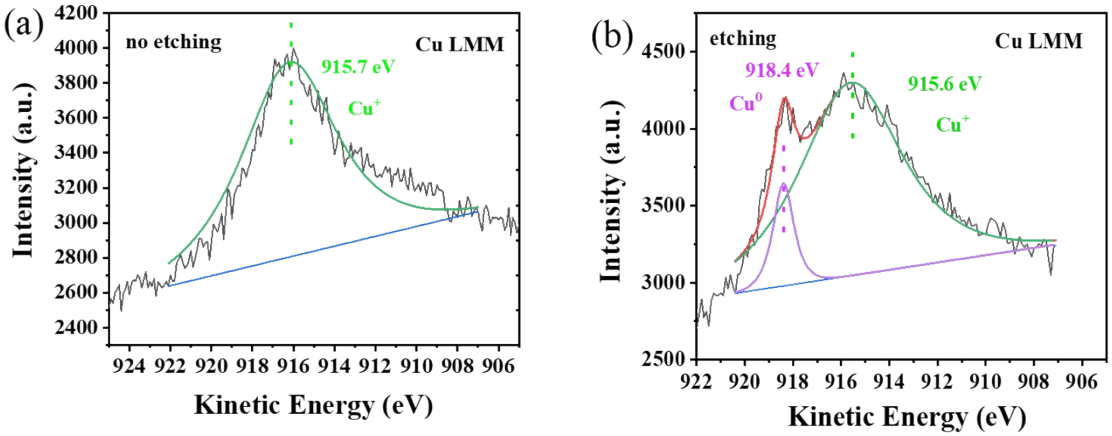

Fig. S14. The used Cu-B_2O_3/PBN Cu 2p XPS for phenol oxidation: (a) unetched and (b) argon ion etching (30 s).

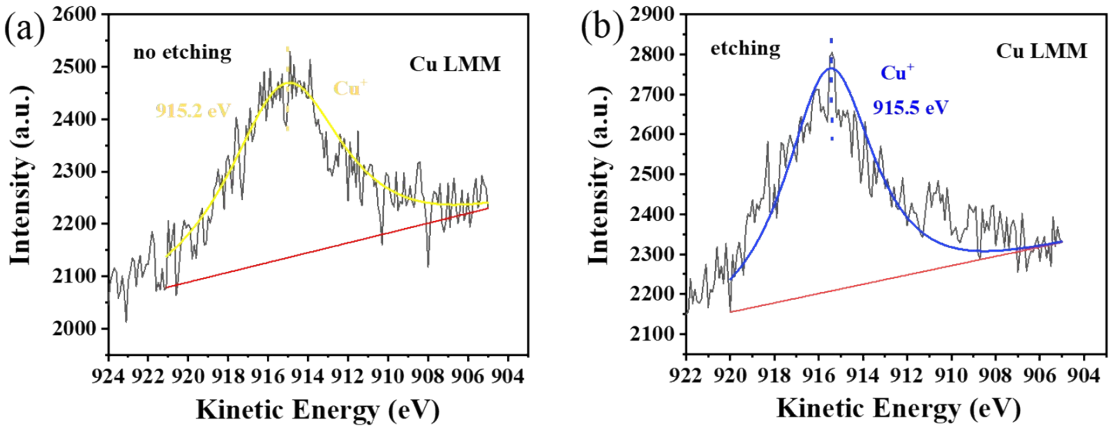

Fig. S15. The used Cu-B_2O_3/PBN Cu 2p XPS for coupling reaction: (a) unetched and (b) argon ion etching (25s).

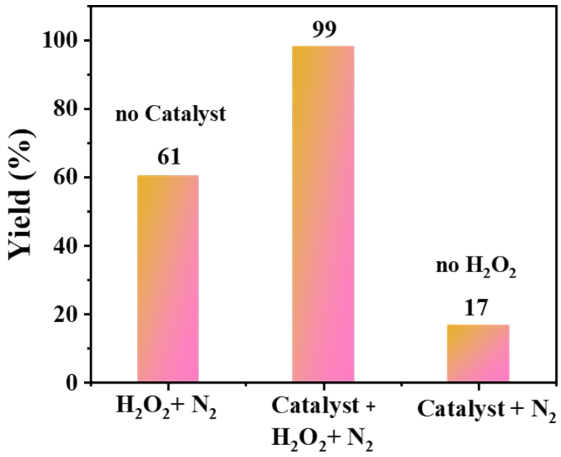

Fig. S16. The yields of phenylboric acid were oxidized to phenol at different conditions.

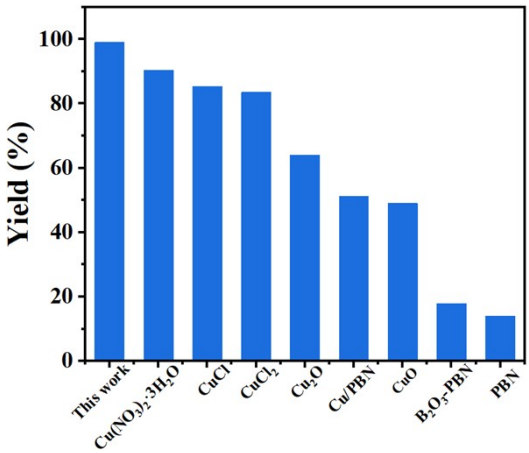

Fig. S17. Heterohydroxylation of arylboric acid on different catalysts.

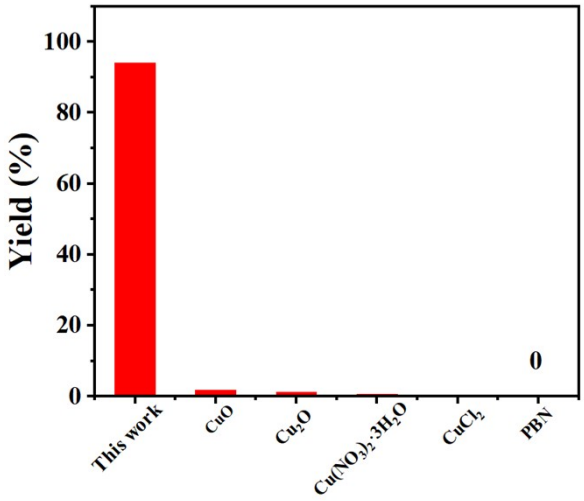

Fig. S18. The C-C homocoupling of aryl boric acid on different catalysts.

Table S1. The effect of reaction time on the yield of electron-withdrawing groups.

Different products	90 min (%)	180 min (%)	300 min (%)	600 min (%)	1200 min (%)
p-methylphenol	28	42	63	74	71
p-methoxyphenol	15	36	45	56	42
p-ethylphenol	12	21	34	37	20
p-chlorophenol	45	69	82	97	94
p-fluorophenol	15	21	37	41	35
1-naphthol	10	0	0	0	0
1-Thiophene	0	0	0	0	0
4-nitrophenol	20	50	85	80	74
4-hydroxybenzonitrile	23	51	88	78	71

Table S2. Catalytic activity comparison of various materials.

Entry	Different catalysts	Catalyst amount	Conditions	Solvent	Yield (%) 	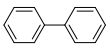	Ref.
1	Cu-B_2O_3/PBN	5 mg	Air, K_2CO_3, 80 ℃, 5 h	H_2O	99	0	This work
			Air, r.t., 5 h	MeOH	3	94	
2	BN-OH	20 mg	H_2O_2, 50 ℃, 30 min	H_2O	95	-	s1
3	graphene oxide	15 mg	H_2O_2, r.t., 10 min	H_2O	99	-	s2
4	Pd/eggshell	3.3 mol%	H_2O_2, r.t., 3 min	-	98	-	s3
5	Ag NPs	0.2 mL (10^{-3} M)	H_2O_2, r.t., 10 min	-	97	-	s4
6	Cu_2O NPs	2 mg	Air, 60 ℃, 5 h	H_2O	100	-	s5
7	CeO_2 nanostructures	10 mg	H_2O_2, r.t., 5 min	H_2O:EtOH =1:1	95	-	s6
8	ZnO NPs	5 mol%	H_2O_2, r.t., 5 min, ultrasonic vibration	H_2O	95	-	s7
9	Cu(II)-based MOF	5 mol%	H_2O_2, r.t., 30 min	H_2O:EtOH =1:1	99	-	s8
10	Fe_2O_3@SiO_2	4 mg	O_2, 50 ℃, 2 h	H_2O	98	-	s9
11	$CuSO_4$-EA	10 mol%	O_2, 60 ℃, 8 h	EtOH	91	-	s10
12	Pd-Chit-CNT	0.5 mol%	H_2O_2, r.t., 15 min	-	97	-	s11
13	Cu@C_3N_4-4	10 mg	Air, r.t., 6 h	H_2O	95		s12
14	Au/MCC	0.0075 mmol	Air, 300 K, 75 min	H_2O	0	98	s13
15	TiO_2-AA-Cu(II)	0.15 mol%	Air, r.t., 1 h	THF	-	95	s14
16	Au-Ag/GO	-	Air, r.t., 1 h	H_2O	-	95	s15
17	CuII/CuI @MIL-101(Cr)	100 mg	Air, r.t.	DMF	-	99.5	s16
18	CuCl	2 mol%	Air, 28 ℃	MeOH	-	93	s17
19	AuNPs.	2 mL	Air, K_2CO_3, 50 ℃, 3 h	EtOH	-	95	s18
20	$Pd(OAc)_2$ /WEPA	1 mol%	Air, r.t., 0.25h	WEPA/ EtOH	-	95	s19
21	Cu(II)-TRIPTA		Air, 60 ℃, 5 h	MeOH	-	96	S20
22	$CuCl_2 \cdot 2H_2O$	5 mol%	Air, r.t., 15 min	MeOH	-	97	s21

Products Characterization

1. Phenol derivatives

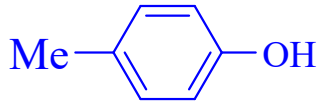

^{1}H NMR (500 MHz, Chloroform-*d*) δ 7.05 (dd, *J* = 8.6, 3.5 Hz), 6.75 (dt, *J* = 8.5, 2.4 Hz), 2.37 – 2.16 (m).

Data are consistent with those reported in *Appl. Catal., A* 2013, 466, 60-67.

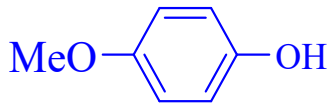

^{1}H NMR (500 MHz, Chloroform-*d*) δ 6.92 – 6.68 (m), 6.05 – 4.52 (m), 3.77 (d, *J* = 2.2 Hz).

Data are consistent with those reported in *Appl. Catal., A* 2013, 466, 60-67.

^{1}H NMR (500 MHz, DMSO-d_6) δ 9.08 (s, 1H), 7.02 – 6.93 (m, 2H), 6.66 (dd, *J* = 8.5, 2.1 Hz, 2H), 2.47 (t, *J* = 7.6 Hz, 2H), 1.12 (t, *J* = 7.5 Hz, 3H).

Data are consistent with those reported in *J. Organomet. Chem.* 2017, 851, 52-56.

^{1}H NMR (500 MHz, DMSO-d_6) δ 9.66 (s, 1H), 7.24 – 7.14 (m, 2H), 6.81 – 6.72 (m, 2H).

Data are consistent with those reported in *J. Organomet. Chem.* 2017, 851, 52-56.

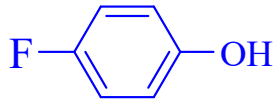

^{1}H NMR (500 MHz, DMSO-d_6) δ 9.34 (s, 1H), 7.00 – 6.93 (m, 2H), 6.78 – 6.67 (m, 2H).

Data are consistent with those reported in *J. Organomet. Chem.* 2017, 851, 52-56

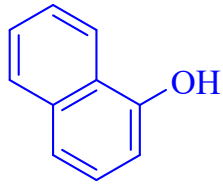

^{1}H NMR (500 MHz, DMSO-d_6) δ 10.10 (s, 1H), 8.17 – 8.10 (m, 1H), 7.80 (dd, J = 7.6, 1.5 Hz, 1H), 7.45 (dddd, J = 16.6, 8.2, 6.8, 1.5 Hz, 2H), 7.36 – 7.25 (m, 2H), 6.88 (dd, J = 7.1, 1.3 Hz, 1H).
Data are consistent with those reported in *ACS Appl. Mater. Interfaces* 2023, 15 (7), 9412-9420.

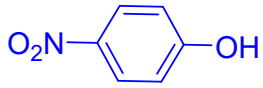

^{1}H NMR (500 MHz, Chloroform-*d*) δ 8.22 – 8.13 (m, 2H), 6.97 – 6.88 (m, 2H), 5.79 (s, 1H).
Data are consistent with those reported in *ACS Omega* 2022, 7, 42126-42137.

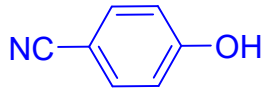

^{1}H NMR (500 MHz, Chloroform-*d*) δ 7.65 – 7.50 (m, 2H), 6.98 – 6.85 (m, 2H), 6.45 (s, 1H).
Data are consistent with those reported in *Lett. Org. Chem.* 2022, 19, 902-907.

2. diphenyl derivatives

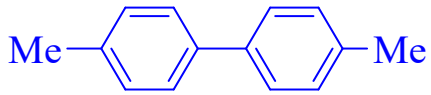

^{1}H NMR (500 MHz, Chloroform-*d*) δ 7.55 – 7.49 (m, 4H), 7.27 (d, J = 7.9 Hz, 4H), 2.42 (s, 6H).
Data are consistent with those reported in *Mol. Catal.* 2021, 501, 111366.

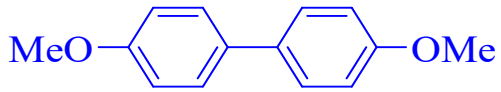

^{1}H NMR (500 MHz, Chloroform-*d*) δ 7.47 (tt, J = 8.1, 3.4 Hz, 2H), 7.33 – 7.28 (m, 2H), 7.26 (t, J = 2.0 Hz, 2H), 7.02 (dd, J = 8.3, 2.9 Hz, 2H), 4.02 – 3.93 (m, 6H), 3.92 – 3.88 (m, 1H).
Data are consistent with those reported in *Mol. Catal.* 2021, 501, 111366.

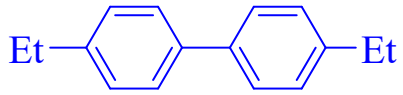

^{1}H NMR (500 MHz, Chloroform-*d*) δ 7.63 – 7.47 (m, 4H), 7.30 (dt, J = 36.2, 7.6 Hz, 4H), 2.74 (ddd, J = 28.3, 14.9, 7.4 Hz, 4H), 1.39 – 1.25 (m, 6H).
Data are consistent with those reported in *Green Chem.* 2014, 16 (6), 2865-2875.

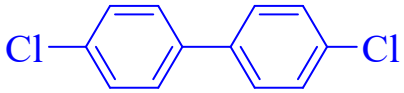

^{1}H NMR (500 MHz, Chloroform-*d*) δ 7.50 – 7.44 (m, 4H), 7.43 – 7.38 (m, 4H).

Data are consistent with those reported in *Green Chem.* 2014, 16 (6), 2865-2875.

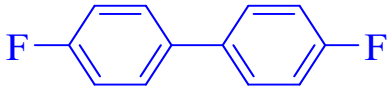

^{1}H NMR (500 MHz, Chloroform-*d*) δ 7.53 – 7.47 (m, 4H), 7.16 – 7.10 (m, 4H).

Data are consistent with those reported in *Green Chem.* 2014, 16 (6), 2865-2875.

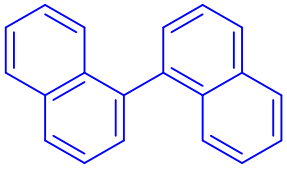

^{1}H NMR (500 MHz, Chloroform-*d*) δ 7.98 – 7.93 (m, 4H), 7.60 (dd, *J* = 8.3, 6.9 Hz, 2H), 7.48 (ddd, *J* = 15.6, 7.5, 1.2 Hz, 4H), 7.41 – 7.38 (m, 2H), 7.29 (ddd, *J* = 8.3, 6.7, 1.3 Hz, 2H).

Data are consistent with those reported in *J. Org. Chem.* 2003, 68 (26), 10130-10134.

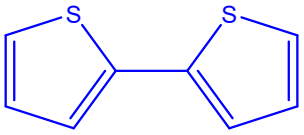

^{1}H NMR (500 MHz, DMSO-d_6) δ 7.49 (dd, *J* = 5.1, 1.2 Hz, 2H), 7.29 (dd, *J* = 3.5, 1.2 Hz, 2H), 7.08 (dd, *J* = 5.1, 3.6 Hz, 2H).

Data are consistent with those reported in *Mol. Catal.* 2021, 501, 111366.

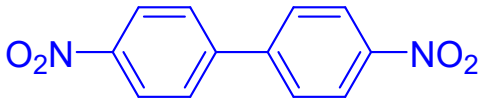

^{1}H NMR (500 MHz, Chloroform-*d*) δ 8.36 (d, *J* = 8.1 Hz, 4H), 7.79 (d, *J* = 8.2 Hz, 4H).

Data are consistent with those reported in *Mol. Catal.* 2021, 501, 111366.

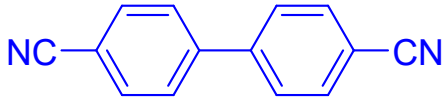

^{1}H NMR (500 MHz, Chloroform-*d*) δ 7.82 – 7.75 (m, 4H), 7.74 – 7.62 (m, 4H).
Data are consistent with those reported in *Green Chem.* 2014, 16 (6), 2865-2875.

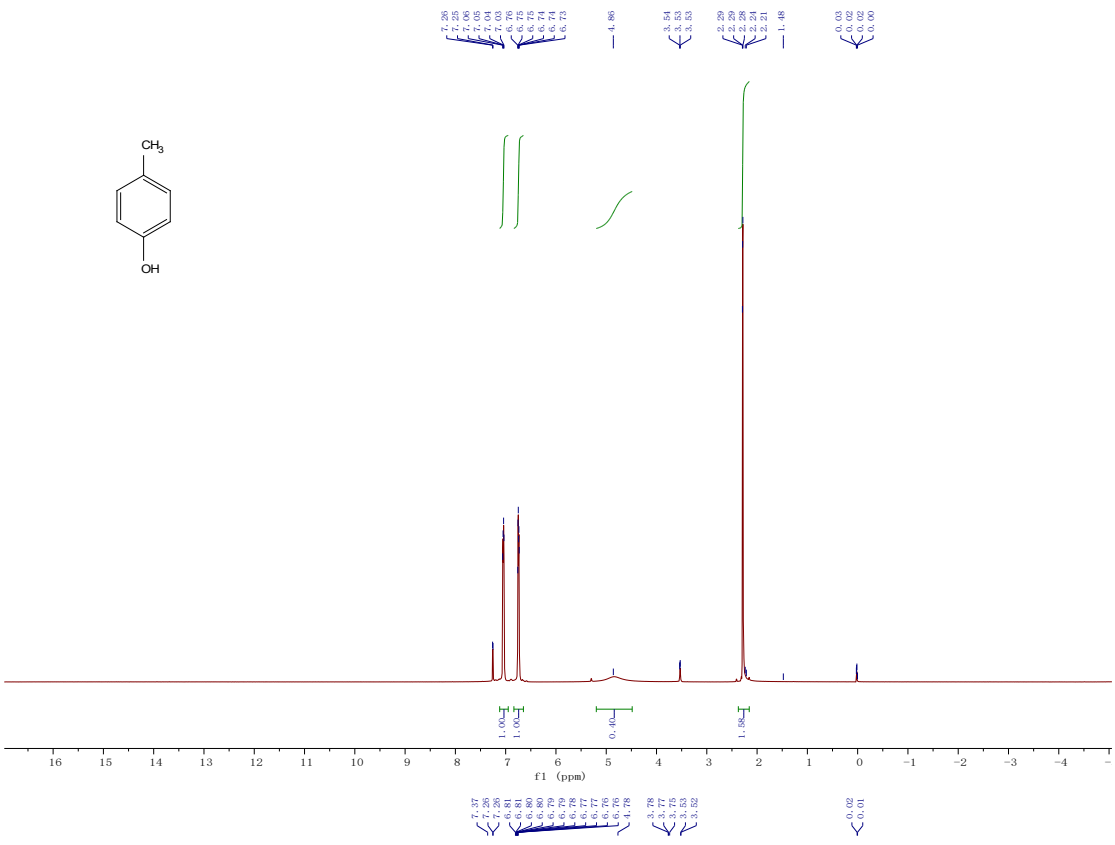

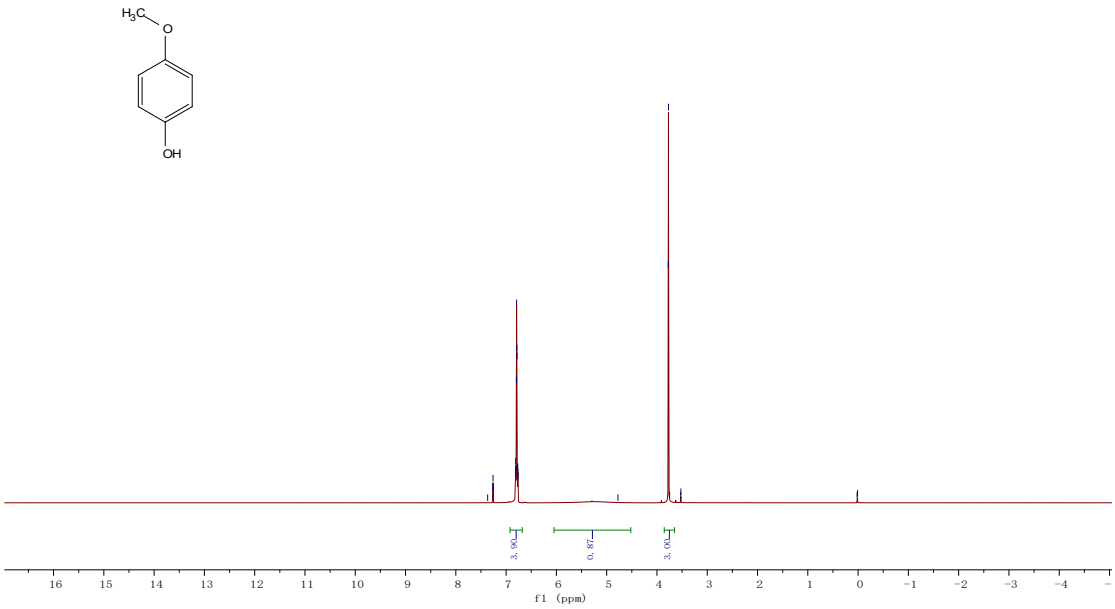

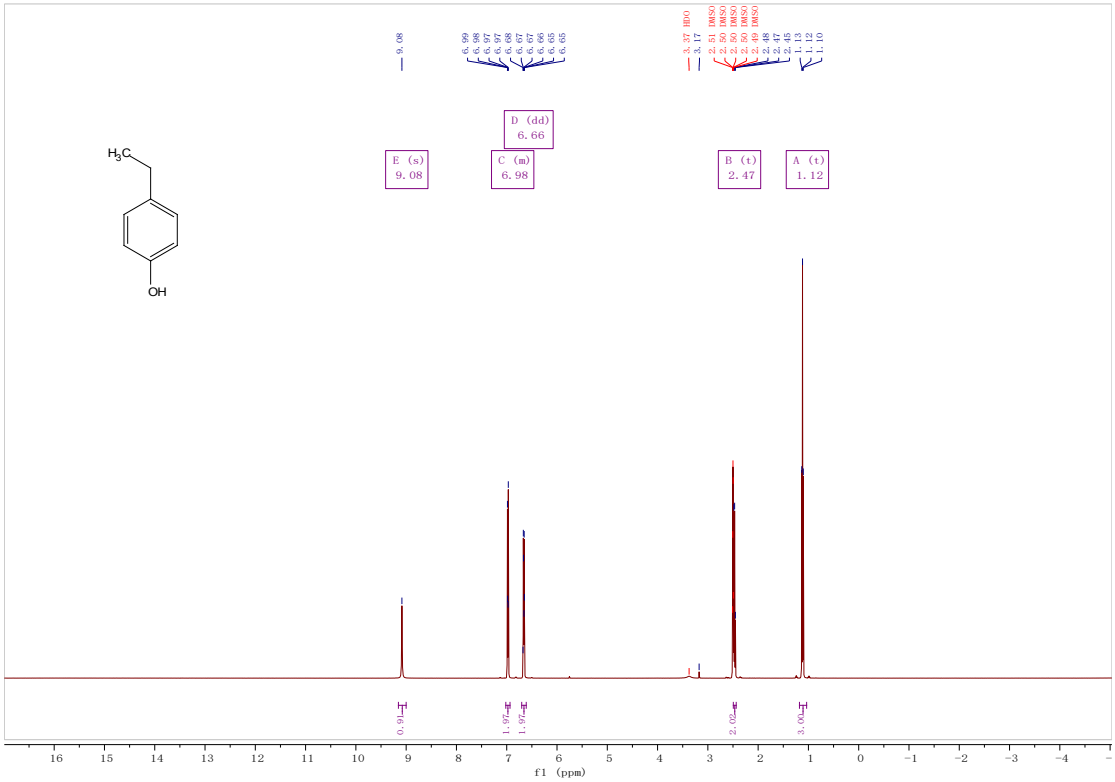
9.08
6.99
6.98
6.97
6.97
6.68
6.67
6.67
6.66
6.65
6.65
3.37 HDO
3.17
2.51 DMSO
2.50 DMSO
2.50 DMSO
2.49 DMSO
2.48
2.47
2.45
1.13
1.12
1.10
H3C
OH
E (s)
9.08
D (dd)
6.66
C (m)
6.98
B (t)
2.47
A (t)
1.12
0.91
1.97
1.97
2.02
3.00
f1 (ppm)

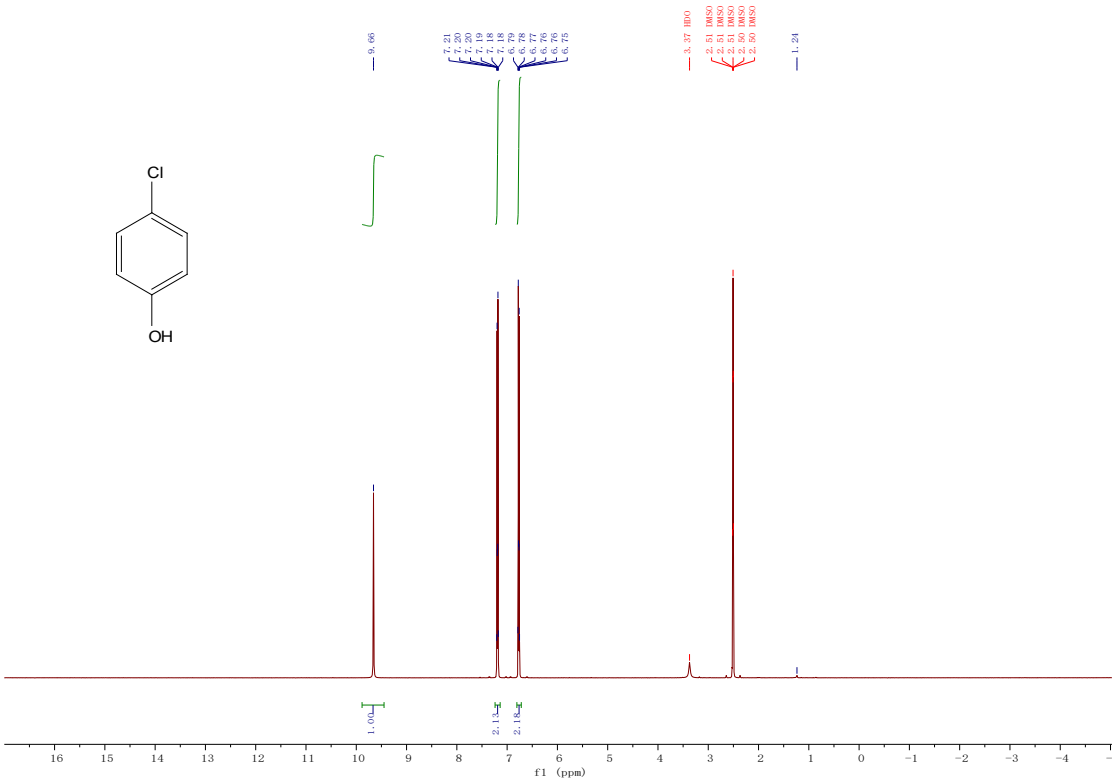
9.66
7.21
7.20
7.20
7.19
7.18
7.18
6.79
6.78
6.77
6.76
6.76
6.75
3.37 HDO
2.51 DMSO
2.51 DMSO
2.50 DMSO
2.50 DMSO
1.24
Cl
OH
1.00
2.13
2.18
f1 (ppm)

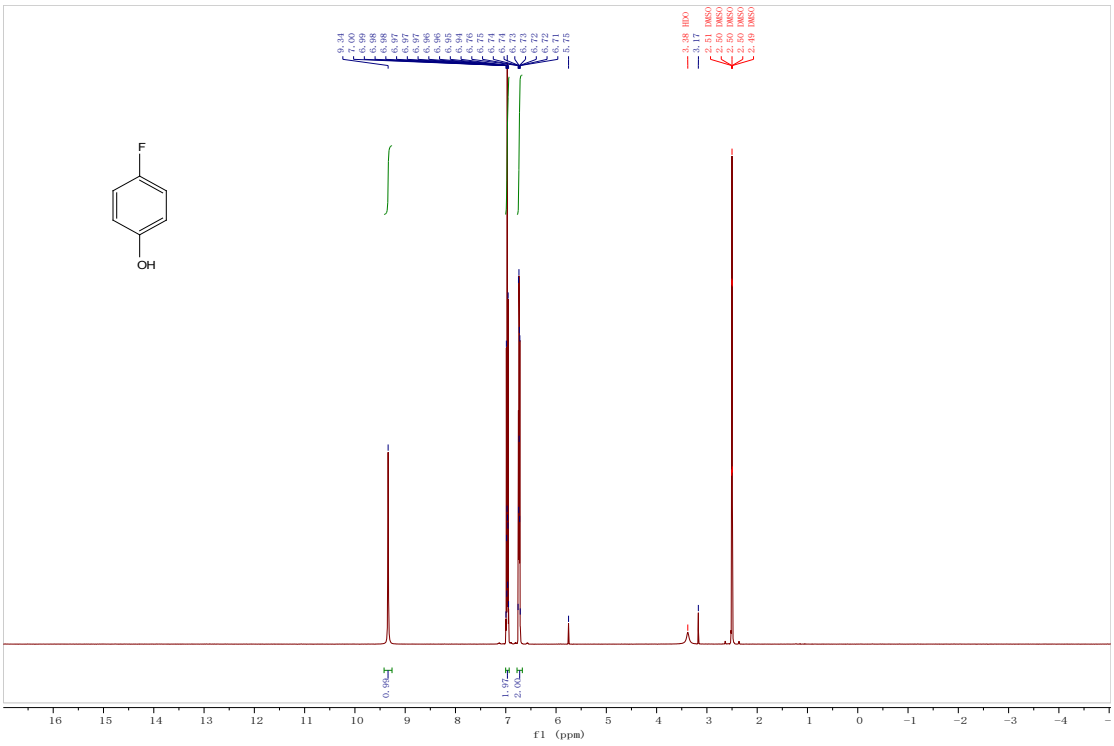
F
OH
9.34
7.00
6.99
6.98
6.98
6.97
6.97
6.97
6.96
6.96
6.95
6.95
6.94
6.76
6.75
6.74
6.74
6.73
6.73
6.72
6.72
6.71
5.75
3.38 HDO
3.17
2.51 DMSO
2.50 DMSO
2.50 DMSO
2.50 DMSO
2.49 DMSO
0.98
1.97
2.00
f1 (ppm)

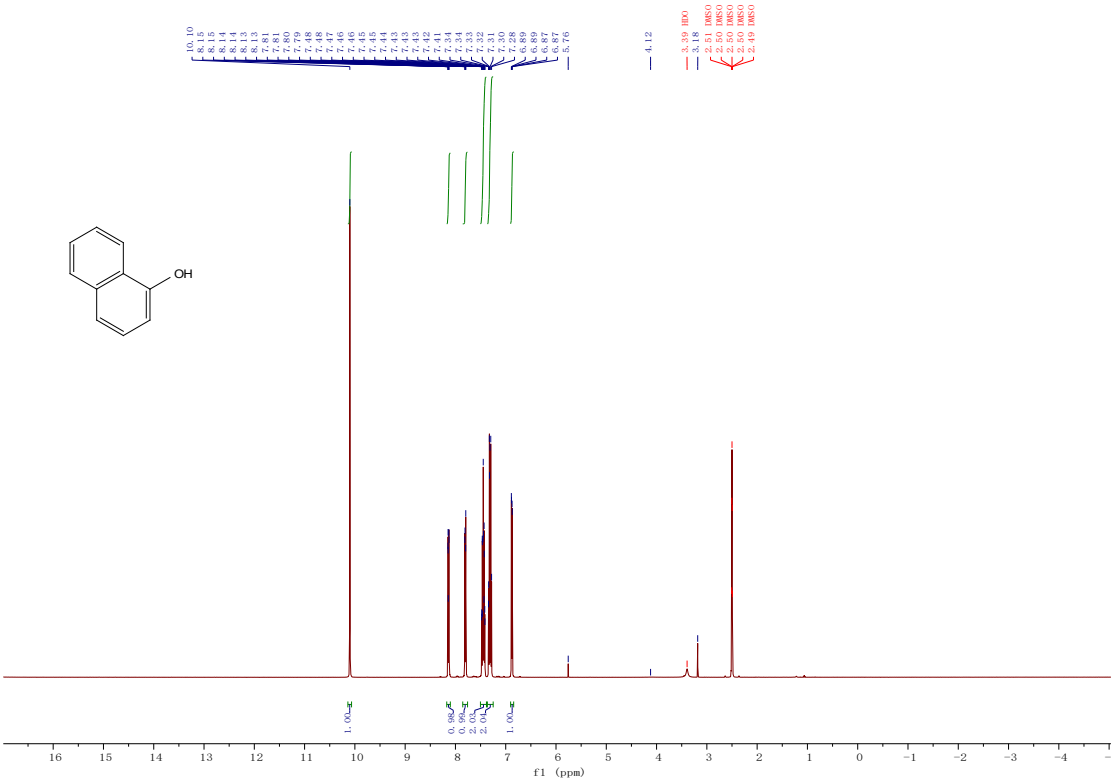
OH
10.10
8.15
8.15
8.14
8.14
8.13
8.13
7.81
7.80
7.79
7.48
7.48
7.47
7.46
7.46
7.45
7.45
7.44
7.43
7.43
7.43
7.42
7.41
7.34
7.34
7.33
7.32
7.31
7.30
7.28
6.89
6.89
6.87
6.87
5.76
4.12
3.39 HDO
3.18
2.51 DMSO
2.50 DMSO
2.50 DMSO
2.50 DMSO
2.49 DMSO
1.00
0.98
0.96
2.03
2.01
1.00
f1 (ppm)

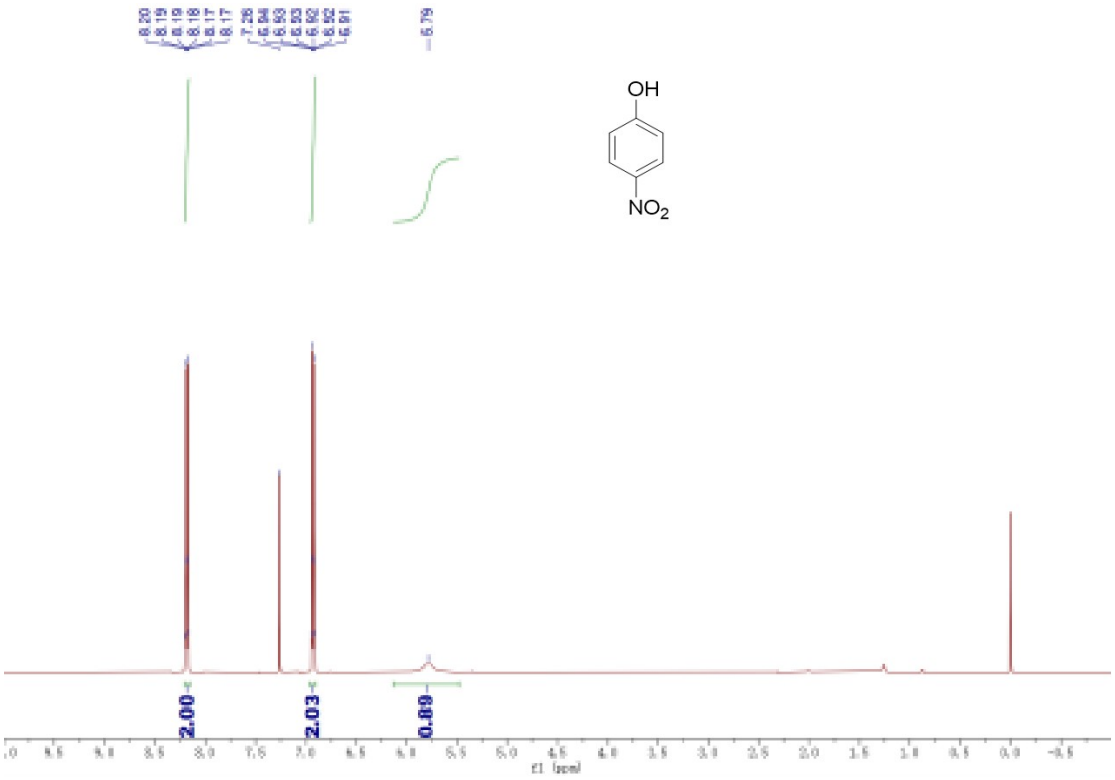
8.20
8.19
8.19
8.18
8.17
8.17
7.26
6.93
6.93
6.92
6.92
6.91
5.79
OH
NO2
2.00
2.03
0.89
f1 (ppm)

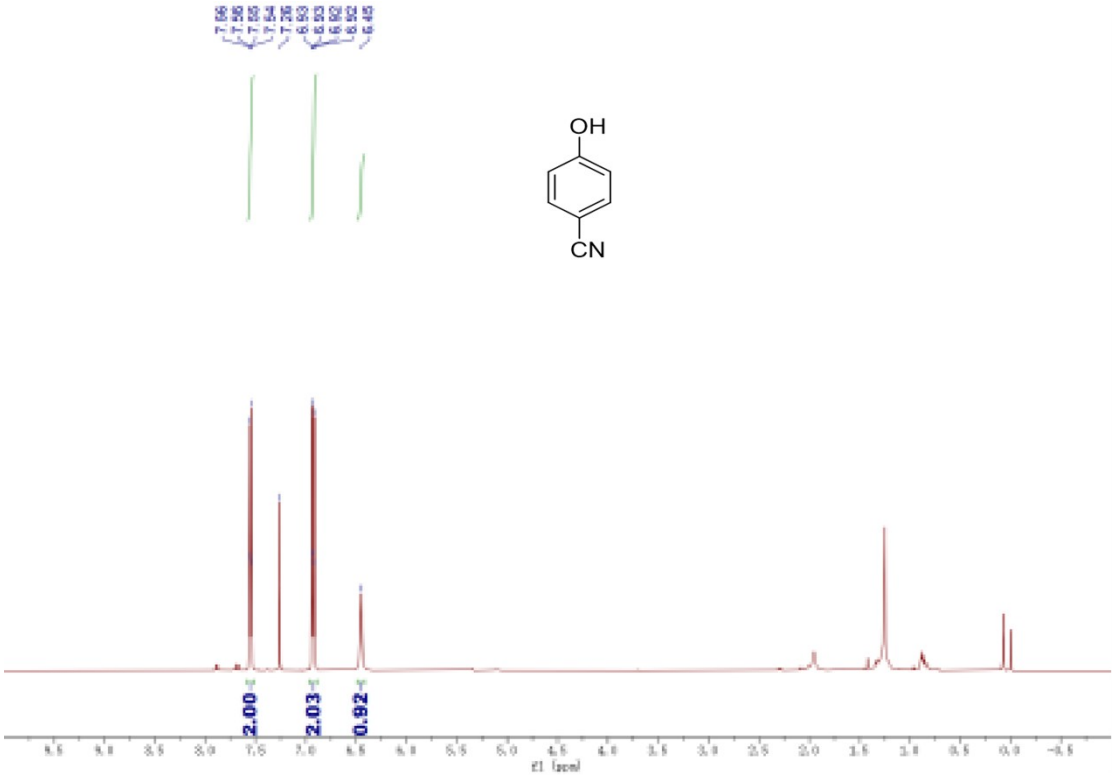
7.56
7.55
7.55
7.54
7.26
6.93
6.93
6.92
6.92
6.45
OH
CN
2.00
2.03
0.92
f1 (ppm)

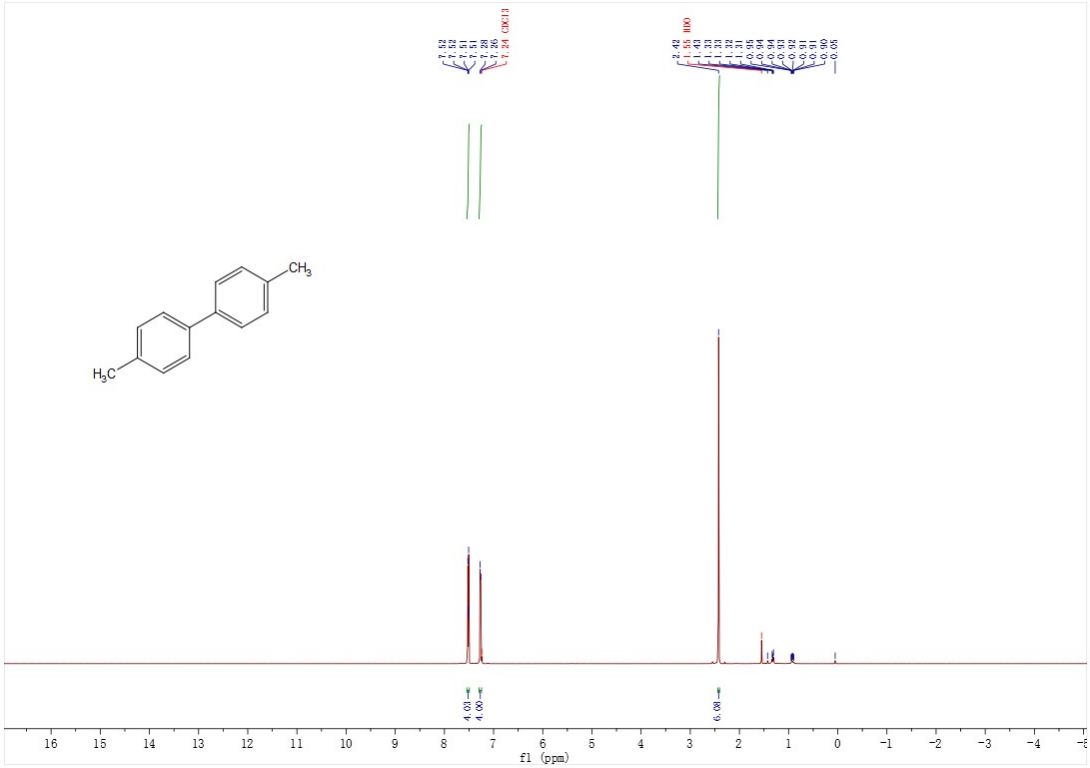
CH3
H3C
f1 (ppm)

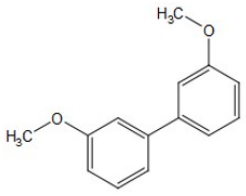
H3C
O
H3C
O

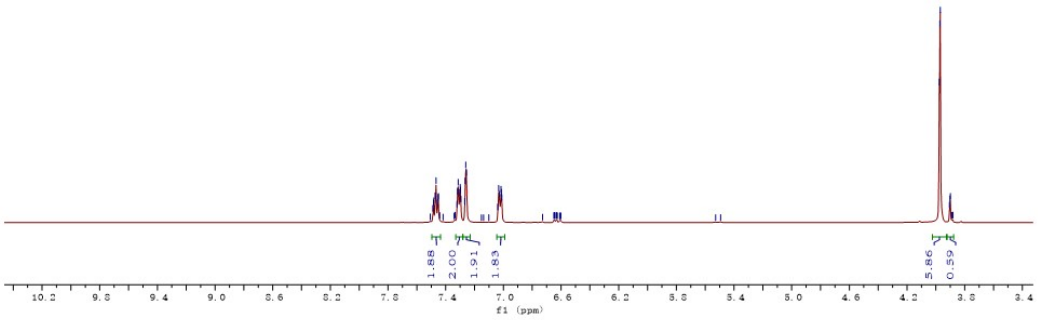
f1 (ppm)

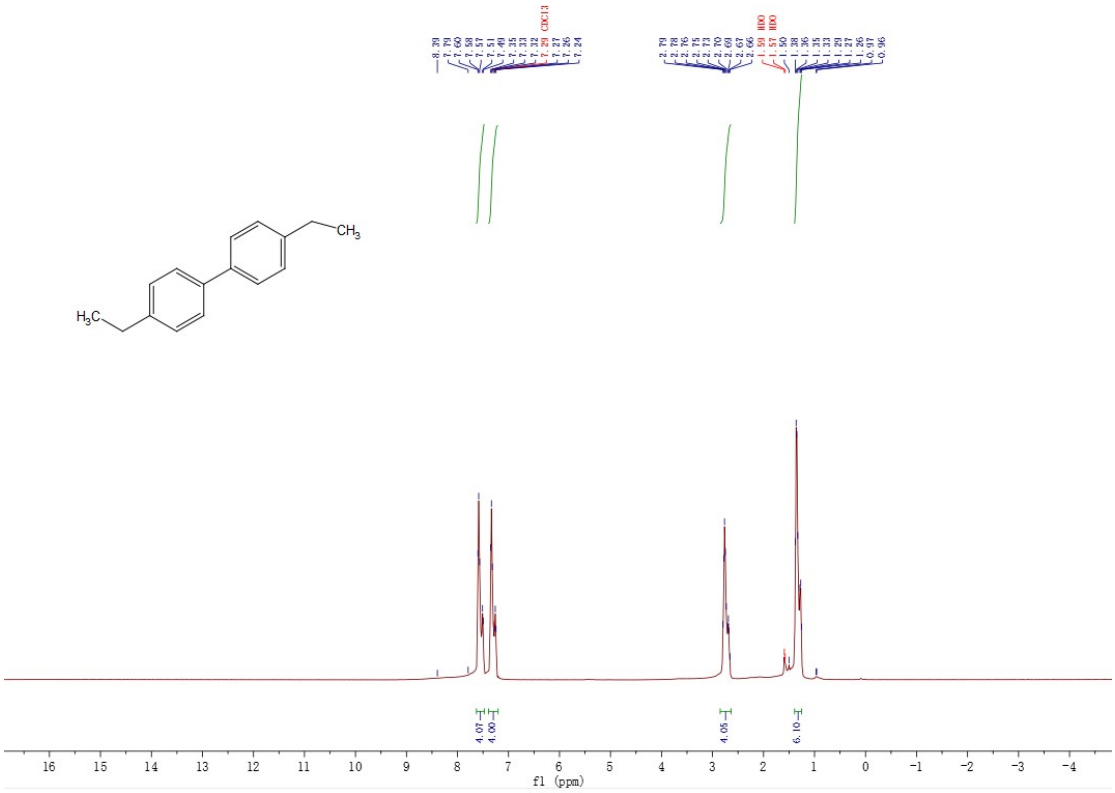
CDCl3
CH3
H3C
4.07
4.00
4.05
6.10
f1 (ppm)

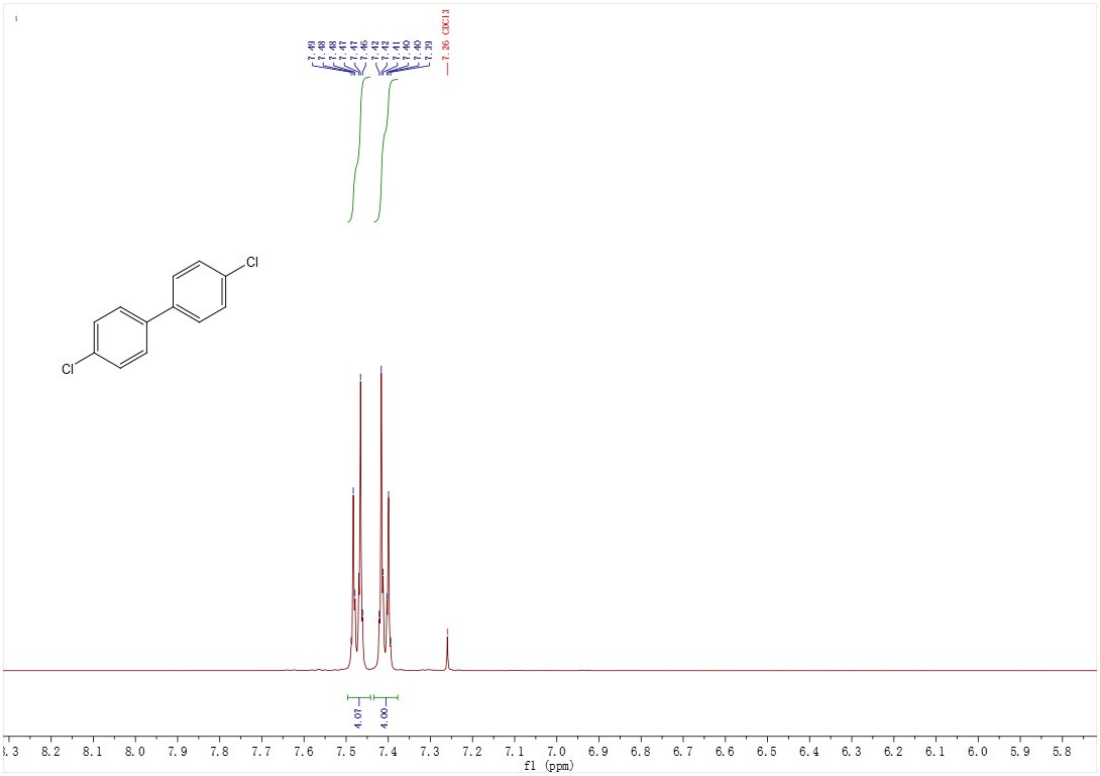
CDCl3
Cl
Cl
4.07
4.00
f1 (ppm)

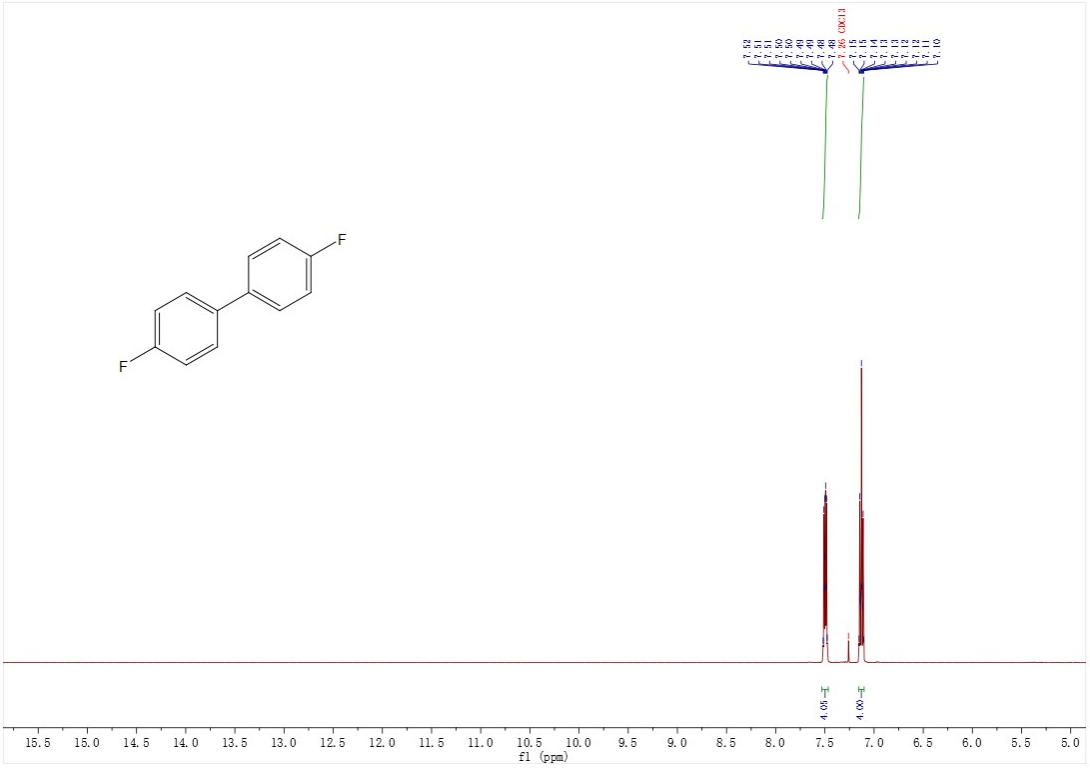
F
F
CDCl3
4.05
4.00
f1 (ppm)

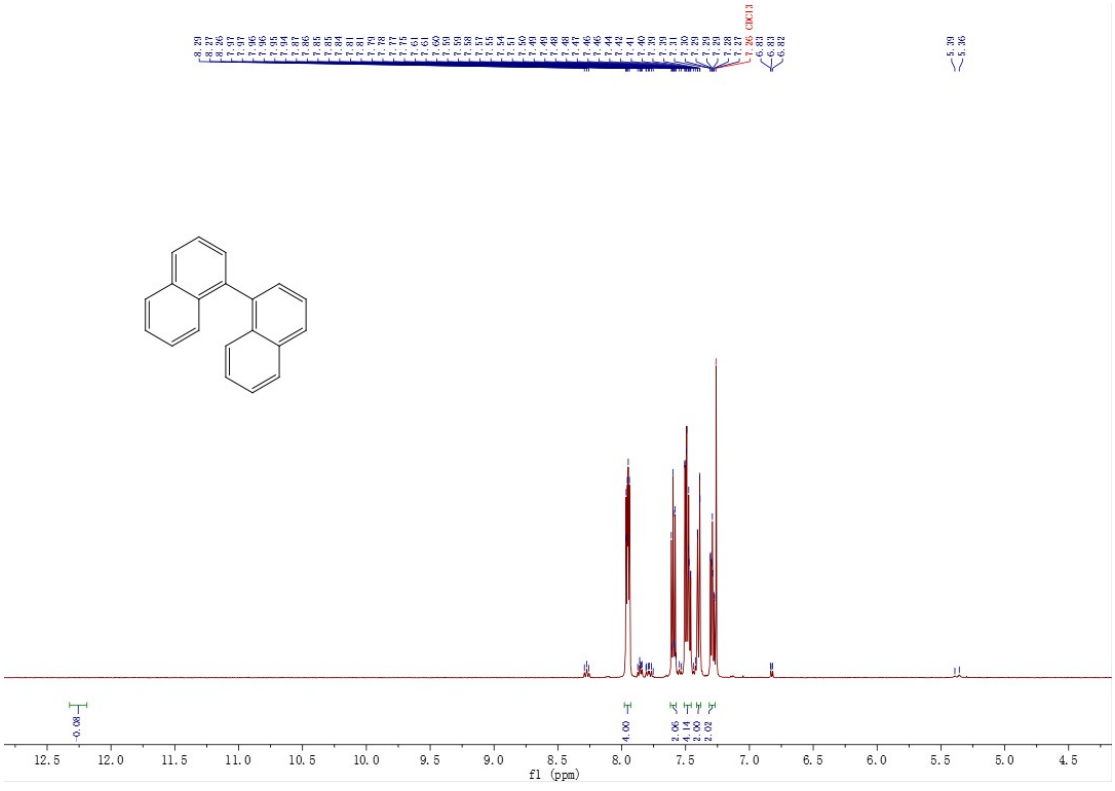
CDCl3
0.08
4.00
2.06
4.00
2.00
f1 (ppm)

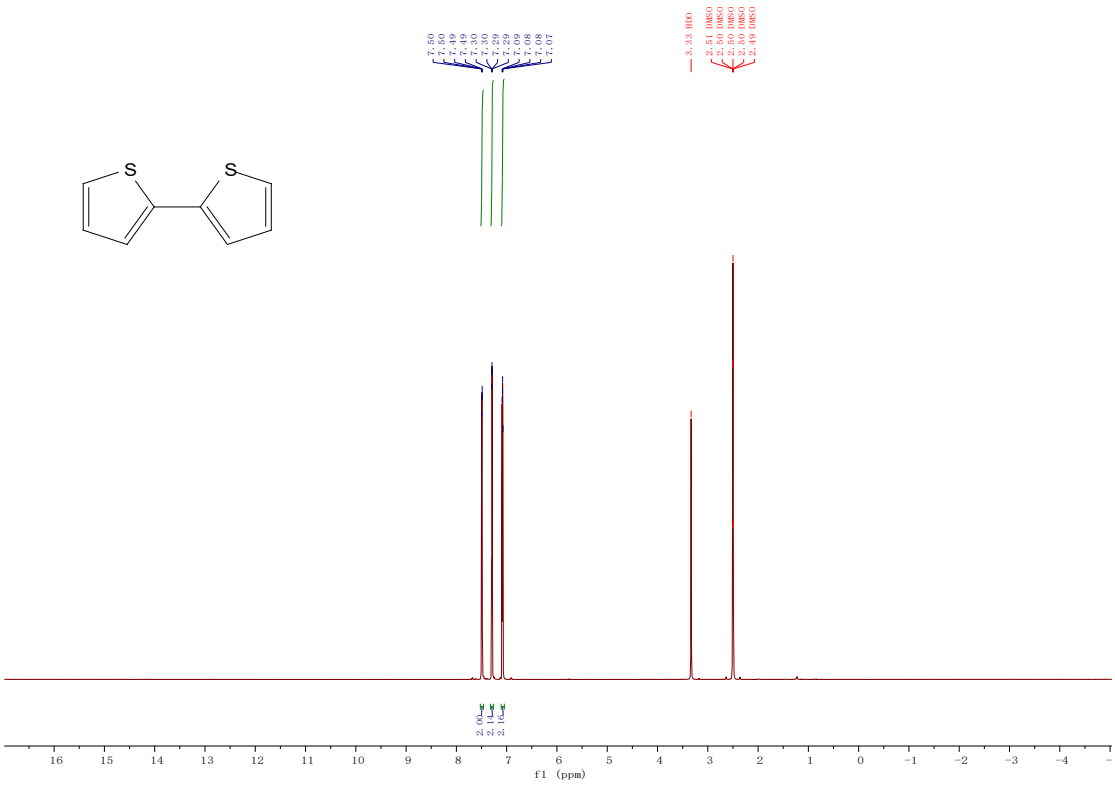
S
S
7.50
7.50
7.49
7.49
7.30
7.30
7.29
7.29
7.09
7.08
7.08
7.07
3.33 HDO
2.51 DMSO
2.50 DMSO
2.50 DMSO
2.50 DMSO
2.49 DMSO
2.00
1.14
2.16
f1 (ppm)

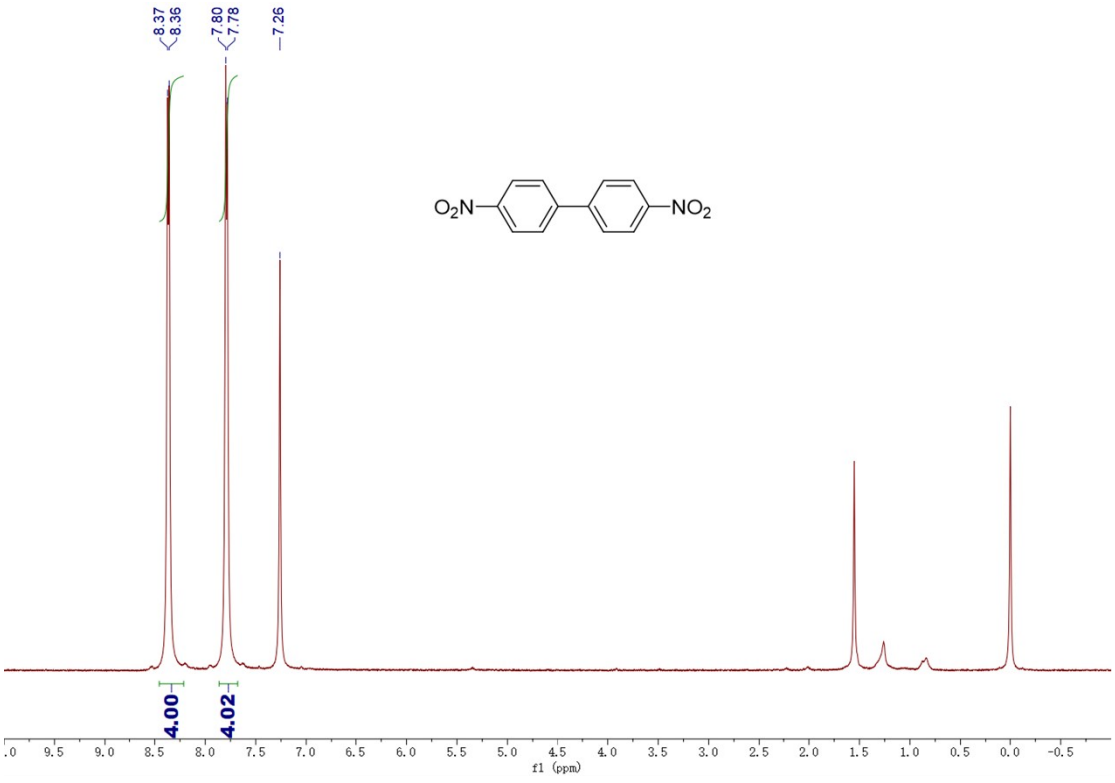
8.37
8.36
7.80
7.78
7.26
O2N
NO2
4.00
4.02
f1 (ppm)

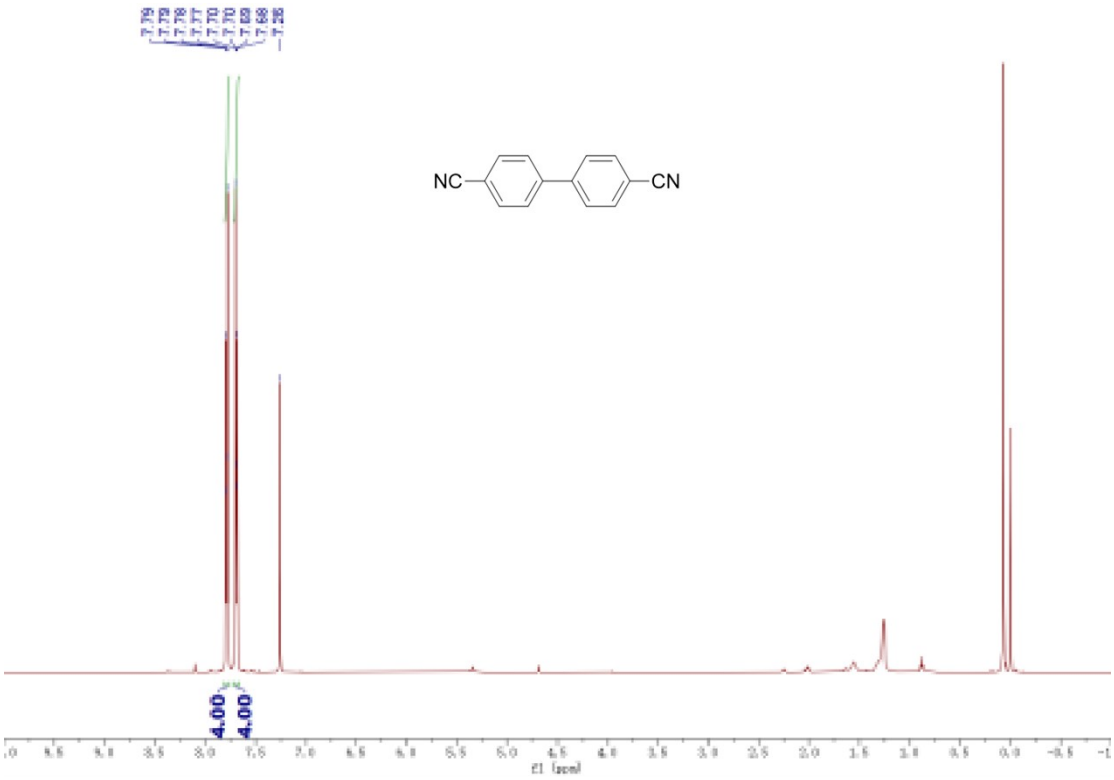
NC
CN
4.00
4.00
f1 (ppm)

References：

s1. P. Choudhary, K. Kumari, D. Sharma, S. Kumar and V. Krishnan, *ACS Appl. Mater. Interfaces*, 2023, **15**, 9412-9420.

s2. M. Karthik and P. Suresh, *ACS Sustainable Chem. Eng.*, 2019, **7**, 9028-9034.

s3. M. Khazaei, A. Khazaei, M. Nasrollahzadeh and M. R. Tahsili, *Tetrahedron*, 2017, **73**, 5613-5623.

s4. V. Kandula, U. Nagababu, M. Behera, S. Yennam and A. Chatterjee, *J. Saudi Chem. Soc.*, 2019, **23**, 711-717.

s5. R. Borah, E. Saikia, S. J. Bora and B. Chetia, *RSC Adv.*, 2016, **6**, 100443-100447.

s6. T. Chandra Saikia, X. Borgohain, S. Iraqui and M. H. Rashid, *ACS Omega*, 2022, **7**, 42126-42137.

s7. T. C. Saikia, S. Iraqui and M. H. Rashid, *Sustainable Chem. Pharm.*, 2022, **25**, 100613.

s8. P. Rani, Heena, N. Pundir, Gauri, A. Husain, K. K. Bhasin and G. Kumar, *Eur. J. Inorg. Chem.*, 2023, **26**, e202200654.

s9. I. Saikia, M. Hazarika, N. Hussian, M. R. Das and C. Tamuly, *Tetrahedron Lett.*, 2017, **58**, 4255-4259.

s10. A. Affrose, I. A. Azath, A. Dhakshinamoorthy and K. Pitchumani, *J. Mol. Catal. A: Chem.*, 2014, **395**, 500-505.

s11. E.-J. Shin, H.-S. Kim, S.-R. Joo, S.-H. Lee and S.-M. Park, *Catal. Lett.*, 2019, **149**, 1560-1564.

s12. M. H. Muhammad, X.-L. Chen, Y. Liu, T. Shi, Y. Peng, L. Qu, and B. Yu, *ACS Sustainable Chem. Eng.,* 2020, **8**, 2682-2687.

s13. K. P. Reddy and A. Murugadoss, *Langmuir*, 2022, **38**, 2205-2212.

s14. N. Pourmorteza, M. Jafarpour, F. Feizpour and A. Rezaeifard, *RSC Adv.*, 2022, **12**, 4931-4938.

s15. T. Wu, J. Ma, X. Wang, Y. Liu, H. Xu, J. Gao, W. Wang, Y. Liu and J. Yan, *Nanotechnology*, 2013, **24**, 125301.

s16. H.-Z. Liu, B. Li, H. Luo, X. Qiu, J.-G. Ma and P. Cheng, *Inorg. Chem.*, 2021, **60**, 11626-11632.

s17. G. Cheng and M. Luo, *Eur. J. Org. Chem.*, 2011, 2519-2523.

s18. W. Jang, J. Yun, P. N. Eyimegwu, J. Hou, H. Byun and J.-H. Kim, *Catal. Today*, 2022, **388-389**, 109-116.

s19. R. M. Appa, J. Lakshmidevi, B. R. Naidu and K. Venkateswarlu, *Mol. Catal.*, 2021, **501**, 111366.

s20. S. K. Das, B. K. Chandra, R. A. Molla, M. Sengupta, S. M. Islam, A. Majee and A. Bhaumik, *Mol. Catal.*, 2020, **480**, 110650.

s21. Y.-N. Cao, X.-C. Tian, X.-X. Chen, Y.-X. Yao, F. Gao and X.-L. Zhou, *Synlett*, 2016, **28**, 601-606.